

Accuracy of low-dose rubidium-82 myocardial perfusion imaging for detection of coronary artery disease using 3D PET and normal database interpretation

Tyler Kaster, BSc, Ilias Mylonas, MD, Jennifer M. Renaud, MSc, George A. Wells, PhD, Rob S. B. Beanlands, MD, and Robert A. deKemp, PhD,

Background. Our aim was to develop a normal database to be used for quantification of myocardial perfusion and diagnosis of “obstructive coronary artery disease” (CAD) using low-dose rubidium-82 three-dimensional (3D) positron emission tomography (PET)-CT.

Methods. From a record of 1,501 patients, 77 were identified as having low-likelihood (LLK) of CAD. Forty LLK patients were used to construct a normal database using 4DM-PET, the remainder used for validation of normalcy. A group of 70 patients with CAD who had invasive coronary angiography and PET-CT were used to evaluate the accuracy of the database for detecting CAD using the sum-stress-score. The effect of clinical exclusion criteria and the inclusion of LLK patients were evaluated.

Results. The normal database for CAD detection had a normalcy rate of 95%. Sensitivity was 100% for detecting patients with either 50% or 70% stenosis. Optimal specificity was 87% for either 50% or 70% stenosis. For localizing disease at 50% stenosis in the left anterior descending, left circumflex, and right coronary artery, sensitivity ranged from 59% to 68%, while specificity was maintained at 87-89%. Similarly, at 70% stenosis, sensitivity ranged from 64% to 79%, and specificity from 87% to 91%.

Conclusions. A normal database containing the relative perfusion scores of patients with LLK of CAD can be used to accurately diagnose obstructive coronary disease using low-dose Rb-82 with 3D PET-CT imaging. (J Nucl Cardiol 2012;19:1135-45.)

Key Words: PET-CT • myocardial perfusion imaging • normal relative perfusion • coronary artery disease • quantification

INTRODUCTION

Myocardial perfusion imaging using Rb-82 positron emission tomography (PET) is a powerful tool for diagnosing obstructive coronary artery disease (CAD) because of its consistently high accuracy.¹⁻⁶ Technological improvements are incrementally improving the

diagnostic ability of PET systems, such as three-dimensional (3D) coincidence detection. 3D PET imaging poses a challenge because of increased scatter; however, this can be outweighed by advantages from the increased sensitivity and count density, which results in improved image quality and reduced patient doses.⁷⁻⁹

Previous studies have described the development of “normal databases” characterizing relative perfusion data for patients with a low-likelihood (LLK) of CAD.^{2,6,10-13} These databases objectively define the normal range of relative perfusion values to evaluate patients with suspected CAD and determine whether the perfusion distribution is normal or abnormal. These databases can be used as an adjunct to the subjective visual scan interpretation by the clinician. Most of the previous studies that have developed LLK normal databases have done so only in the context of SPECT or 2D PET myocardial perfusion imaging. There is a need for the development of additional LLK normal

See related editorial, pp. 1110-1112

From The National Cardiac PET Centre and Cardiac Research Methods Centre, Division of Cardiology, University of Ottawa Heart Institute, Ottawa, ON, Canada.

Received for publication Apr 11, 2012; final revision accepted Aug 28, 2012.

Reprint requests: Robert A. deKemp, PhD, The National Cardiac PET Centre and Cardiac Research Methods Centre, Division of Cardiology, University of Ottawa Heart Institute, 40 Ruskin Street, Ottawa, ON K1Y 4W7, Canada; radekemp@ottawaheart.ca.

1071-3581/\$34.00

Copyright © 2012 American Society of Nuclear Cardiology.

doi:10.1007/s12350-012-9621-y

databases for 3D Rb-82 PET MPI. The objective of this study is to describe the development of such a database using 3D hybrid PET-CT imaging, and evaluate its accuracy for the diagnosis of CAD.

METHODS

Patients

LLK normals. Using a record of 1,501 patients who underwent PET perfusion scans between July 2009 and December 2010 (inclusive), a group of patients with a LLK of CAD was identified. This group was created by removing any patient with the following: known CAD [i.e., previous myocardial infarction (MI), percutaneous coronary intervention (PCI), and CABG], typical or atypical angina, diabetes, and rest or stress ECG interpreted as anything other than “normal.” Contrary to Bateman et al,¹ abnormal scan interpretation was not incorporated as an exclusion criterion, because the PET scans were also used subsequently to evaluate normalcy. For each LLK patient, the Morise pre-test risk score (0-24) was computed based on common cardiac risk factors (age, gender, obesity, diabetes, smoking, hypertension, hyperlipidemia, family history, and angina symptoms).¹⁴ It is comparable to the Diamond and Forrester criteria,¹⁵ but accounts for additional cardiac risk factors including estrogen status in females, and is applicable to patients with or without angina symptoms. Only patients with a Morise score which classified them as low (0-8) or medium (9-16) pre-test probability of having CAD were included. This resulted in a total of 77 patients (34 males, 43 females) who were considered within the LLK group. As Morise score stratifies patients into risk levels rather than providing a numerical probability of CAD, the mean Diamond-Forrester pre-test probability was also calculated to quantitatively verify that these patients did in fact have a low pre-test probability of CAD.

Normal database. Out of the 77 patients, 20 male and 20 female patients were randomly selected from the eligible LLK group with scans acquired on the Discovery 690 PET-CT system (GE Healthcare, Milwaukee, WI) used currently in our institution. These 40 patients were used to create the normal database. Normalcy of these patients was evaluated using the same normal database for disease detection in patients, as internal validation initially.

Validation of normal database. Of the remaining 37 patients, one patient with BMI of 58 was excluded because of a poor quality CT attenuation scan resulting in a significant perfusion artifact. As external validation, the 36 remaining LLK patients were used to evaluate normalcy as a surrogate for specificity of disease detection.

Coronary angiography patients. Using the same record of 1,501 patients, two angiography cohorts were defined using patients who had invasive coronary angiography (ICA) within 6 months following PET. The “general” patient cohort (n = 70) had no history of CABG, and no PCI <6 months before PET. As a subset of the general cohort, the “standard” angiography cohort (n = 45) also excluded patients with acute

intervened MI (n = 7) or left ventricular ejection fraction (LVEF) <40% (n = 18) because of the known effect of cardiomyopathy on perfusion independent of obstructive epicardial coronary disease, following the methods of Bateman et al.¹ History of acute intervened MI was defined as any patient treated with PCI or thrombolytics immediately following any previous MI. There were no patients with MI in the interval between PET imaging and catheterization.

Protocols

Myocardial perfusion imaging. As described previously,¹⁶ patients were instructed to fast overnight, and abstain from caffeine for 12 hours, and theophylline drugs for 48 hours before the MPI scan. Anti-anginal medications (β -blockers, calcium blockers, and nitrates) were withheld on the morning of the test. Following patient positioning on the scanner bed, a normal-end-expiration low-dose (0.4 mSv) fast helical (1.5 seconds) x-ray CT scan was acquired for attenuation correction (AC) of the PET scan. A custom elution system (RbES; Jubilant DraxImage, Kirkland, QC) was used for delivery of a 30-second constant-activity-rate infusion of 10 MBq/kg of Rb-82 (Ruby-Fill(TM); Jubilant DraxImage, Kirkland, QC). This system produces a consistent square-wave activity profile injection regardless of the age of the generator, resulting in consistent scan timing, count-rates and image contrast between patients.^{17,18} The perfusion scan was started 2 minutes after the initial arrival of activity in the scanner field of view. Therefore, using this 30-second tracer infusion protocol, the perfusion data were acquired starting approximately 90 seconds after the end-of-infusion, similar to ASNC standard guidelines.¹⁹ An 8-minute ECG-gated scan was acquired in 3D-mode, using the Discovery RX or 690 PET-CT 64-slice scanner (GE Healthcare, Milwaukee, WI). ECG-gating was performed with 8 bins per cycle, heart-rate-adaptive binning, and bad-beat rejection at 80 beats per minute \pm 50% window. Three minutes following dipyridamole infusion (0.14 μ g/kg/minute \times 5 minutes), stress imaging was performed using the same protocol described above at rest. Aminophylline (150 mg over 3 minutes) was administered starting 7 minutes following the end of dipyridamole stress. A post-stress CT attenuation scan was acquired for AC of the stress data. Review of the PET-CT image alignment for AC was performed for each study manually using the vendor AC quality control program on the scanner console. Any shift greater than 3 mm was used for PET-CT re-alignment and reconstruction of the static and gated images. Static and gated images were reconstructed using the vendor OSEM iterative reconstruction (VuePoint HD) with 12 and 16 mm Hann post-filter, respectively. LVEF was measured using 4DM-PET (v2010) clinical interpretation software (INVIA, Ann Arbor, MI) analysis of the stress gated images.²⁰ Transient ischemic dilatation (TID) was estimated from the un-gated static images as the ratio of stress/rest LV endocardial volumes, using 4DM-PET with mid-septal definition of the aortic valve plane.²¹

ICA. Coronary angiography was used as the gold standard for determination of CAD, defined as stenosis \geq 50% or \geq 70%. The stenosis measurements were obtained

from the catheterization reports in the patient's medical record. The left anterior descending artery (LAD) was defined as both the proximal and mid LAD as well as the first diagonal. The right coronary artery (RCA) was defined as the proximal and middle RCA. The left circumflex artery was defined as the proximal and middle LCX, the first and second marginal branch of the LCX, as well as the ramus intermedius. Stenosis in the left main artery was considered to be disease in both the LAD and LCX. Stenoses in the distal coronary segments of the LAD/RCA/LCX, subsequent diagonal/marginal branches, posterior descending artery, or postero-lateral segments were not classified as disease because of the expected minor impact that these lesions would have on global and regional perfusion. However, to verify this assumption, we examined the impact on results when distal segments were included.

Disease detection. The sum stress score (SSS) was calculated by a single operator (TK) in a 17-segment model using 4DM-PET clinical interpretation software. The severity of the relative perfusion defects for each segment were defined as follows: 1.5 standard deviations below the mean was equivocal (defect score of 1), 3 standard deviations below the mean was abnormal (defect score of 2), 4.5 standard deviations below the mean was severe (defect score of 3), 6 standard deviations below the mean was absent perfusion (defect score of 4).

The defect scores in each segment were summed to obtain the SSS. Based on the SSS, each patient was classified into one of the following four groups. For a SSS of 0-3, the patient was considered not to have significant disease. The SSS values of

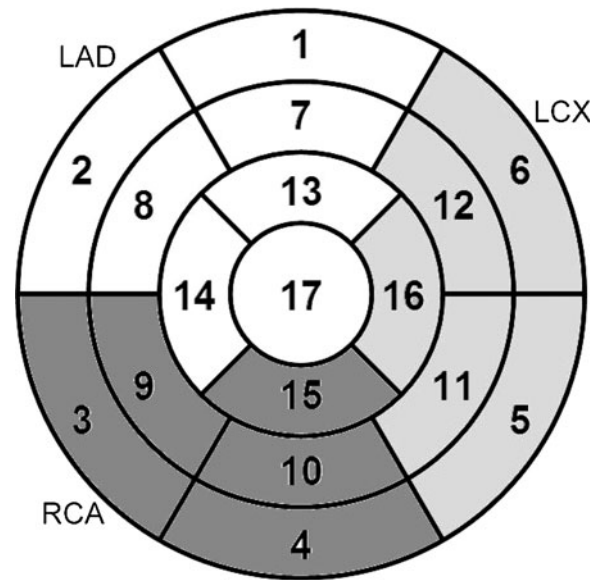


Figure 1. American Heart Association 17-segment model of coronary artery territories²³.

4-7, 8-11, and ≥ 12 were considered mild, moderate, and severe disease, respectively. For this study, a SSS value greater than or equal to 4 from the PET scan was considered to be a "positive" scan, consistent with previous studies by our group and others.^{16,22,23} The cutoff of 1.5 standard deviations below

Table 1. Demographics for each of the three patient groups

	Database normals	Validation normals	Angiogram patients
Number	40	36	70
Age	58.2 ± 10.3 (33-75)	58.7 ± 11.2 (38-82)	63.5 ± 11.7 (33-93)
Male (%)	20 (50.0)	14 (38.9)	51 (72.9) [†]
BMI	31.3 ± 7.4 (20-45)	35.3 ± 8.8 (20-60)	33.2 ± 8.0 (19-56)
Obesity (BMI > 27) (%)	23 (57.5)	26 (72.2)	49 (70.0)
Prior MI (%)	0 (0)	0 (0)	24 (34.3) [†]
Prior PCI (%)	0 (0)	0 (0)	17 (24.3) [†]
Prior PCI and MI (%)	0 (0)	0 (0)	11 (15.7)
Diabetes (%)	0 (0)	0 (0)	30 (42.9) [†]
Smoker (current or past) (%)	26 (65.0)	17 (47.2)	37 (52.9)
Smoker (current) (%)	4 (10)	3 (8.3)	10 (14.3)
Hypertension (%)	14 (35)	17 (47.2)	53 (75.7) [†]
Dyslipidemia (%)	20 (50)	13 (36.1)	51 (72.9) [†]
Family history (%)	16 (40.0)	14 (38.9)	32 (45.7)
Morise risk score	10.5 ± 3.4 (2-16)	9.7 ± 4.1 (2-16)	14.6 ± 3.5 (5-24) [†]
Diamond & Forrester probability CAD (%)	7.45	8.14	46.2 [†]

Continuous measures are presented as mean ± standard deviation (min-max), and used Wilcoxon rank sum tests for analysis. Categorical measures are presented as frequencies with percentages, and used Fisher exact tests for analysis

BMI, Body-mass index; PCI, percutaneous coronary intervention; CAD, coronary artery disease; MI, myocardial infarction

[†] Statistical significance ($P < .05$) vs the validation normals

the mean was chosen to rule out false positive scans with approximately 95% specificity.

TID was used in conjunction with SSS as a marker of CAD to account for the possibility of triple-vessel disease.²¹ If the patients had normal perfusion ($SSS \leq 3$) or mild disease ($4 \leq SSS \leq 7$) as demonstrated by PET perfusion, but had $TID \geq 1.2$, then they were re-classified as moderate disease ($8 \leq SSS \leq 11$). If the patients already had moderate or severe disease ($SSS \geq 12$), then TID was not considered to alter their disease status.

Disease localization. Using the standard American Heart Association 17-segment model, the territories supplied by each major vessel were defined according to Figure 1.²⁴ The cutoff values for localizing disease were the same as those used for global disease (0-3, 4-7, 8-11, and ≥ 12), expecting that global disease should be localized in one of the coronary territories. In each territory, the SSS was calculated and disease status for each of the three territories was determined. The results for localized disease detection were calculated using the standard angiography cohort.

Statistical Analysis

Sensitivity, specificity, accuracy, negative predictive value, positive predictive value, and prevalence were calculated for both 50% and 70% stenosis in both cohorts. Sensitivity and specificity were assessed at mild, moderate, and severe thresholds of disease ($SSS \geq 4, 8, \text{ and } 12$, respectively) to create the receiver operating characteristic (ROC) curves using JROCFIT.²⁵ Optimal sensitivity and specificity were reported at the operating point with $SSS \geq 4$ as the threshold for a positive scan. Comparing the standard cohort with the general cohort allowed us to examine the impact patient selection criteria (specifically LVEF $< 40\%$ and history of intervened MI) on the results. As well, the 36 LLK validation normals were included in a stepwise fashion, to determine their impact on the measured specificity. For the univariate analysis of continuous measures, Wilcoxon rank sum tests were used, while for categorical measures, Fisher exact tests were performed using SAS 9.2 2002-2008 (SAS Institute Inc., Cary, NC). *P* values less than .05 were considered statistically significant.

RESULTS

Demographics

The demographic information (self-reported) in the three patient groups is summarized in Table 1. There were no significant differences in patient characteristics between the database and validation normal groups. The angiogram patients were comparable to the normal groups in terms of age and BMI, but were significantly different ($P < .05$) in terms of cardiac history (MI, PCI) and several risk factors reflected in the increased Morise risk score ($P < .05$). The mean probability of CAD for both the validation and database normal patients was

under 10%, which was significantly different ($P < .05$) from the 46.2% mean for the ICA patients.

Normal Database

There were no significant differences between the segmental perfusion means or variances in men vs women ($P = NS$); therefore, a composite gender database was used. The segmental values of the normal database are presented in Figure 2. The normalcy ($SSS \leq 3$) rate of the normal database was 95.0% (38/40) as expected. The two abnormal scans had $SSS = 4$ and 7. The TID value of all normal database patients was < 1.2 . Normalcy was also assessed for the validation group and was found to be 94.4% (34/36). The two abnormal scans both had $SSS = 5$. The TID values of all validation group patients were < 1.2 .

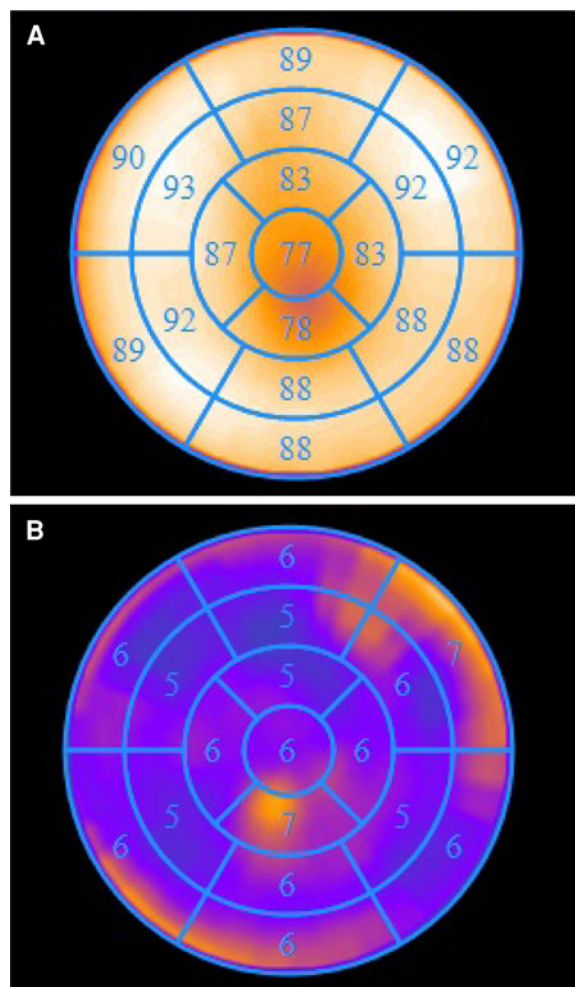


Figure 2. Stress normal database mean (A) and standard deviation (B) polar maps with relative perfusion average values in each segment (%).

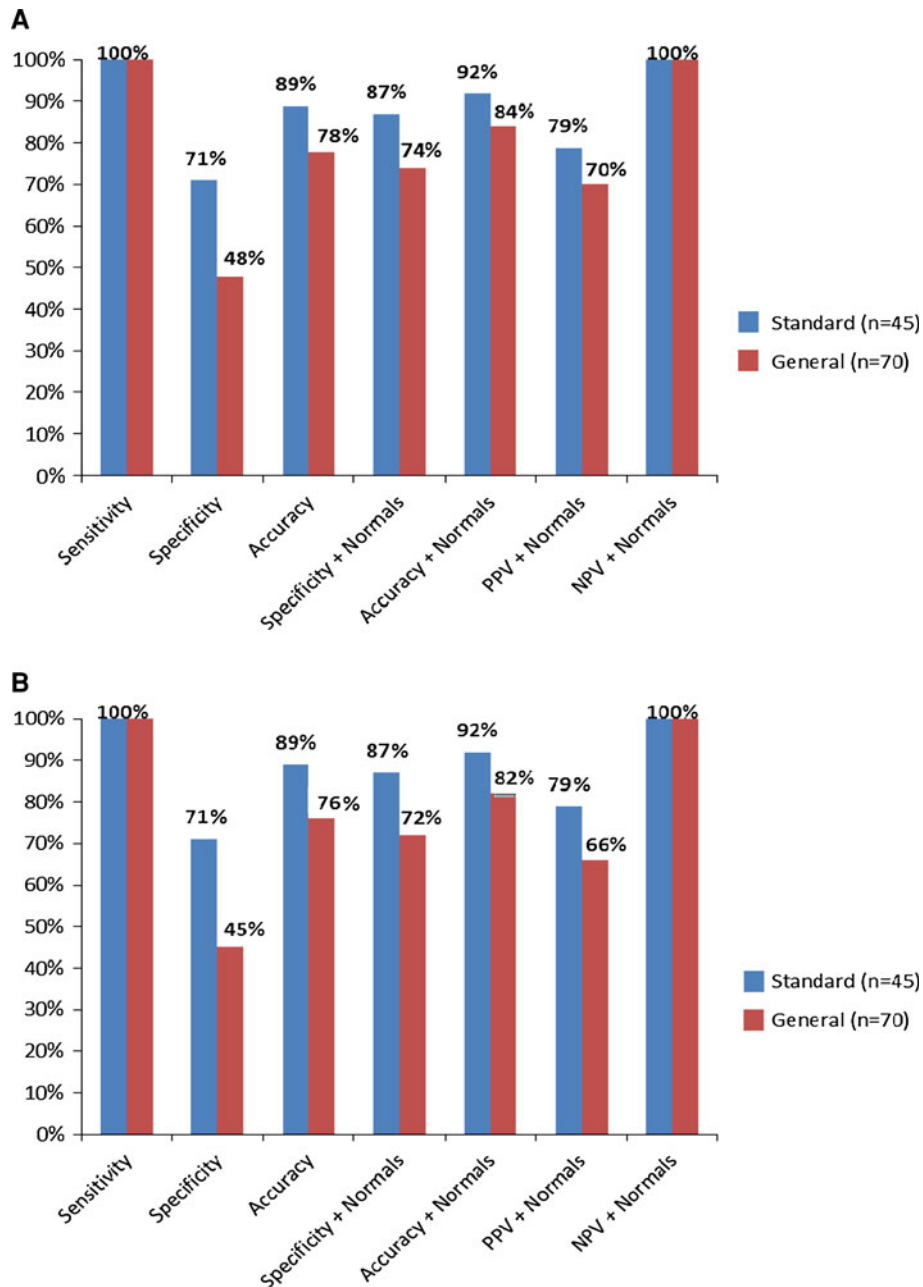


Figure 3. Normal database detection of global obstructive CAD at (A) 50% and (B) 70% stenosis. Standard cohort excluded patients who had PCI within 6 months of PET, any history of CABG, LVEF < 40%, or history of intervened MI. General cohort excluded only patients who had PCI within 6 months of PET, or any history of CABG. “+Normals” indicates the 36 LLK validation normals are included in the reported values. PPV is positive predictive value and NPV is negative predictive value.

Coronary Angiogram Patients

In the general cohort, the prevalence of CAD at 50% stenosis was 58.6% (41/70) and the prevalence at 70% stenosis was 55.7% (39/70). In the standard cohort, the prevalence of CAD at both 50% and 70% stenosis was 62.2% (28/45).

Disease detection. The performance of the 3D PET normal database for detection of global CAD is shown in Figure 3. TID > 1.20 detected CAD accurately in two patients with normal perfusion ($SSS \leq 3$), and reclassified two other patients from mild to moderate disease, resulting in a small increase in sensitivity

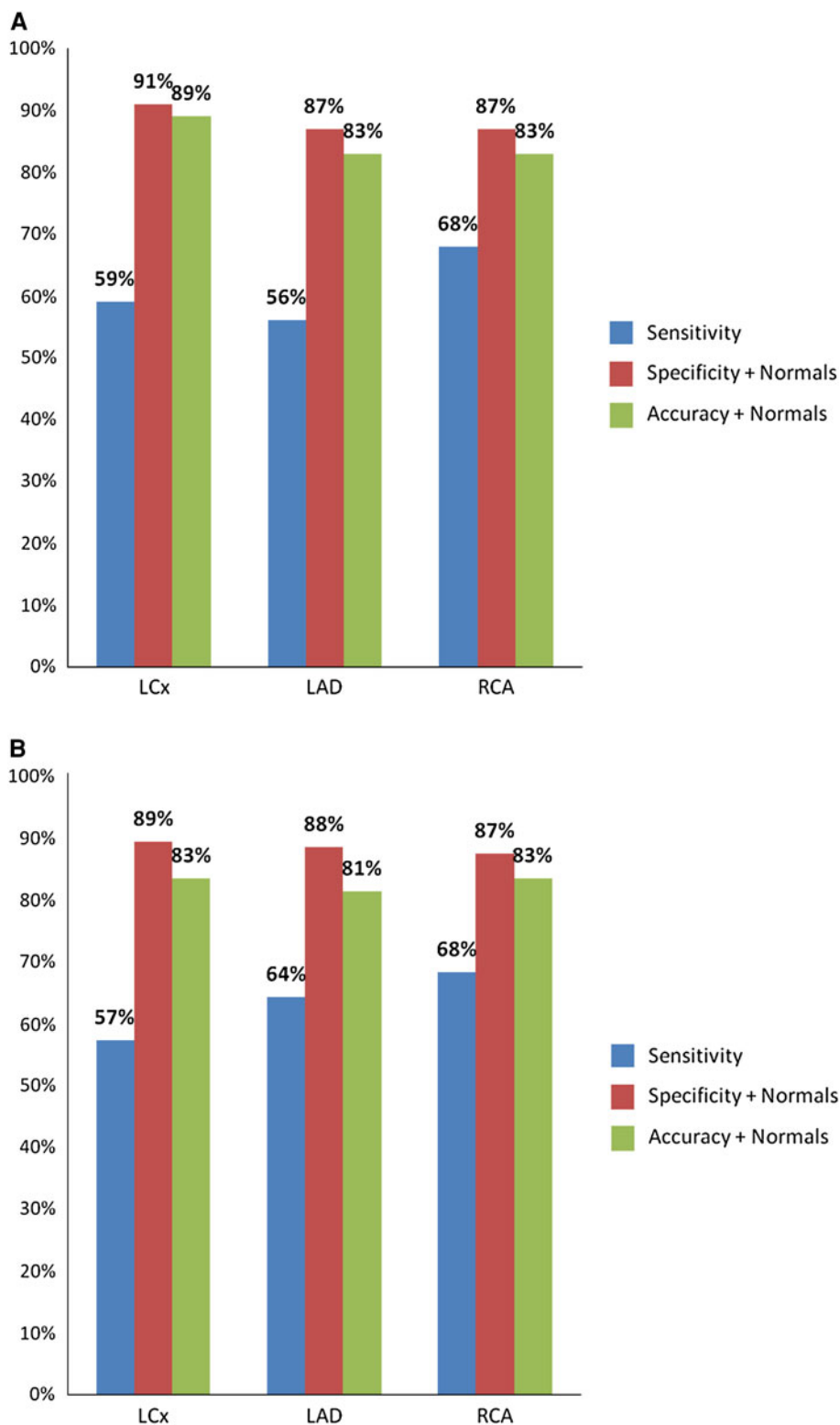


Figure 4. Normal database localization of obstructive CAD at (A) 50% and (B) 70% stenosis. Sensitivity, specificity, and accuracy are presented for each of the three main coronary vessels in the standard cohort. “+Normals” indicates 36 LLK validation patients included in the calculations.

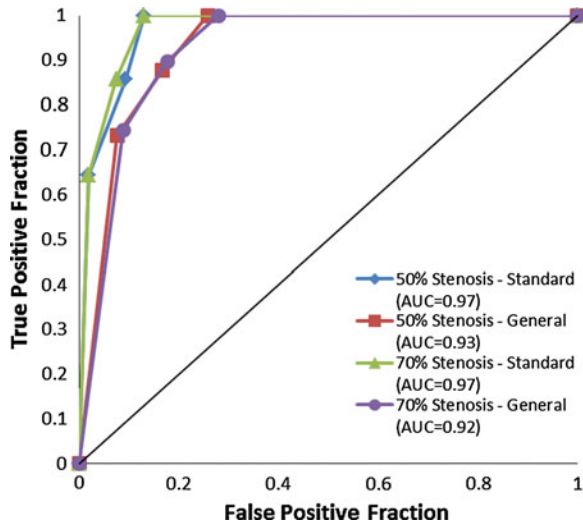


Figure 5. ROC curves for detection of CAD at 50% and 70% stenosis severity. $SSS \geq 4$ was used as the cutoff point for determining the presence of CAD. AUC is area under curve.

from 95% to 100%. There were no false positives as a result of using TID to detect CAD. When distal coronary artery segments of the LAD, LCX, and RCA were included in the definition of disease, at 50% stenosis, there was one additional false positive, and at 70% stenosis there was one additional false positive and one true positive. All other patients were unchanged.

Inclusion of the 36 LLK validation normal patients increased the specificity, accuracy, and PPV as expected. Comparing the general vs standard cohorts, inclusion of patients with LVEF <40% or history of intervened MI appears to worsen outcomes results for both 50% and 70% stenosis disease.

Disease localization. The ability of the normal database to detect localized CAD in each of the three main coronary vessels is illustrated in Figure 4. These results are for the standard angiography cohort, and include the LLK validation patients to calculate specificity. The specificity for detecting the presence of disease in the patient is similar to the specificity of localized disease detection. However, the sensitivity decreases when *localizing* regional disease as opposed to *detection* of the presence or absence of the disease in the patient.

ROC Curves

The performance of the database to detect disease is also illustrated in the ROC curves shown in Figure 5. The AUC in all cases ranges from 0.93 to 0.97. These results include the 36 LLK validation normal in the calculations.

DISCUSSION

This study was performed to develop and validate a normal database for 3D PET-CT myocardial perfusion imaging with low-dose Rb-82. The normalcy rate of the database was measured using a separate validation group of 36 patients with LLK of CAD, matched to the LLK normal database group according to the Morise and Diamond-Forrester criteria (Table 1). The accuracy of this database was then determined by using patients who had had both catheterization as well as 3D PET-CT imaging performed within 6 months. ICA was used as the gold standard for defining patients with and without CAD.

Our method for selecting patients with a LLK of CAD appears accurate. Both the normal database and the validation group of LLK patients had a high rate of normalcy (95.0% and 94.4%, respectively) using the $SSS \leq 3$ and $TID < 1.2$ criteria. This means it is likely our patients in the database did not have CAD. However, having not performed ICA on the LLK patients we cannot definitively say these patients were free from CAD.

The 3D PET normal database was extremely sensitive in detecting CAD (Sensitivity = 100% for both 50% and 70% stenosis). False-positive defects in the relative perfusion distribution may have been produced by non-obstructive heart disease, resulting in a slightly less impressive specificity (87% for 50% and 70% stenosis). Of the 18 patients with LVEF <40%, there were 9 false positives (specificity = 50%), and no false negatives (sensitivity = 100%) at 70% stenosis, consistent with previous findings summarized in the appropriate use criteria.²⁶ Even though patients who had a low ejection fraction were excluded in the standard cohort, this may not necessarily have removed all patients with cardiomyopathies potentially affecting regional myocardial perfusion. The 7 patients with intervened MI accounted for 4 out of 5 false-positive results in the 11 patients with history of prior PCI and MI at 70% stenosis. Some remaining false-positives may be related to the fact that the gold standard ICA used an *anatomical* definition, rather than a *functional* definition of disease, which would be more representative of the perfusion data acquired using PET imaging. Nonetheless, a negative scan appears to be a strong indicator that a patient does not have significant CAD (negative predictive value = 100%). Our results may also have been affected by our definition of disease on angiography, as we did not incorporate distal coronary arteries or the numerous other diagonal/marginal branches into our definition of disease. However, it was found that the impact on results was minimal given that at both 50%

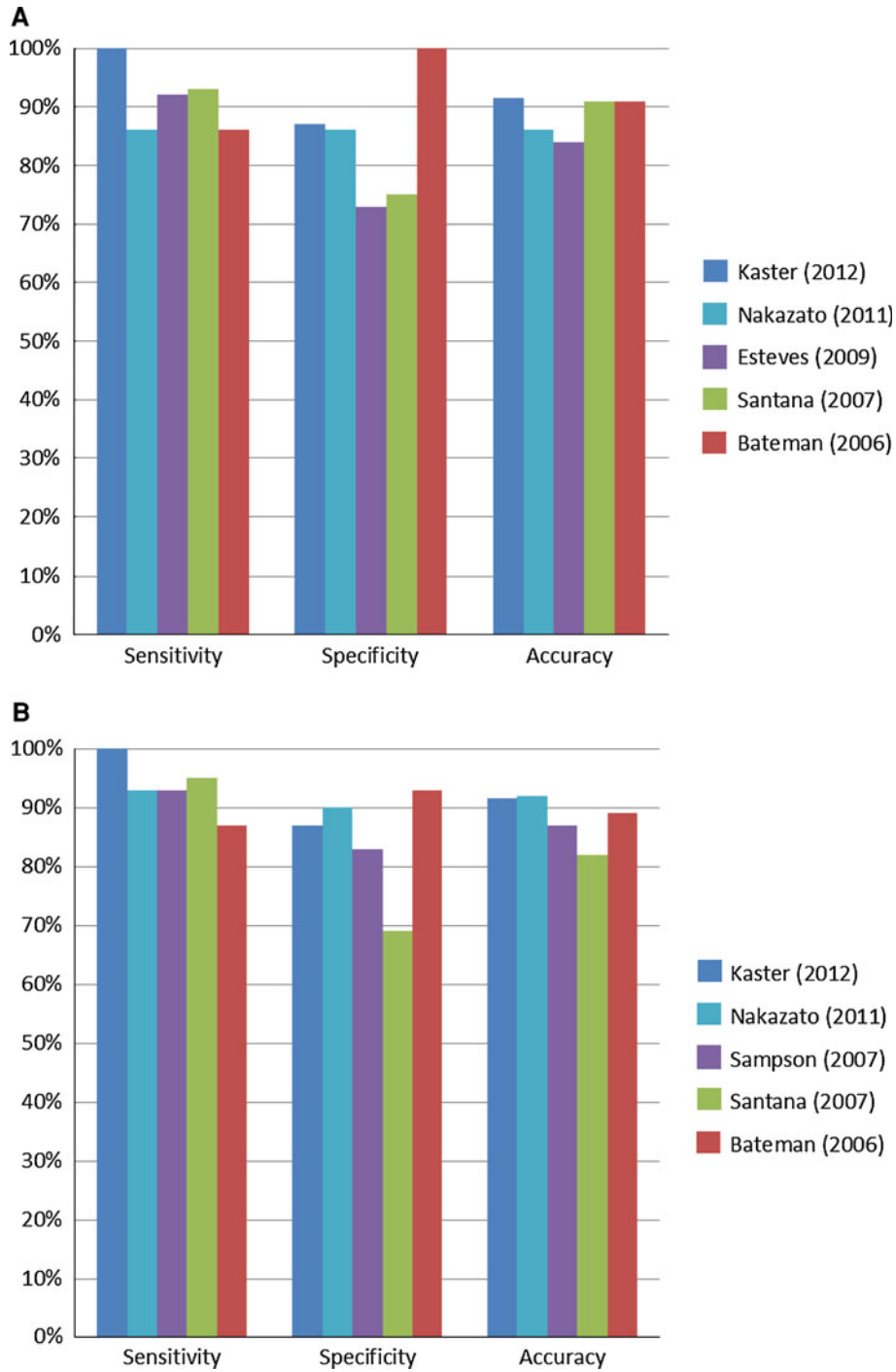


Figure 6. Previous studies examining accuracy of PET/CT systems at (A) 50% stenosis and (B) 70% stenosis. The present study is shown for the standard cohort.

and 70% stenosis there was only one additional false positive, and one true positive at 70% stenosis.

A decrease in sensitivity was observed when localizing disease. While specificity remained relatively

constant (87-88%) the sensitivity was reduced when localizing disease (mean of 63%) compared to detection (100%). This is partly due to the discrete mapping of polar map segments to coronary artery territories, which

Table 2. Selection criteria used in rubidium-82 PET-CT diagnostic accuracy studies

	2D or 3D imaging	Database or expert visual interpretation	LLK normals included	Prior PCI excluded	Prior MI excluded	LVEF < 40% excluded
Kaster (present study)	3D	Database	Yes and no	<6 months	Intervened MI	Yes and no
Nakazato et al ⁶	3D	Database	No	Yes	Yes	Non-ischemic cardiomyopathy
Esteves et al ³	2D	Expert visual and database	No	No	Yes	No
Santana et al ²	2D	Database	No	No	No	No
Sampson et al ⁴	2D	Expert visual	Yes	Yes	Yes	No
Bateman et al ¹	2D	Expert visual	Yes	No	Intervened MI	Yes

PCI, Percutaneous coronary intervention; MI, myocardial infarction; LVEF, left ventricular ejection fraction

does not always reflect the individual patient anatomy accurately. When disease occurs it is often, but not always localized exactly within the coronary artery territories assigned to the discrete polar map segments. For example, a stenosis in the LAD could, because of anatomical variation, create a perfusion defect on the PET image that spans both the LAD and RCA coronary artery polar map territory. The global disease will be detected, however, the SSS threshold may not be met in any one individual coronary artery territory on the polar map. This can result in false negatives, which may explain the reduced sensitivity in disease localization. This decrease in sensitivity for localizing disease is also a limitation of *relative* perfusion imaging generally, e.g., if one focal region of the myocardium has severely decreased perfusion relative to the maximum which is *also reduced* below normal, then the extent and severity of disease will be under-estimated. Sensitivity for multi-vessel disease detection and localization may be improved with *quantitative* perfusion (myocardial blood flow) imaging.²⁷⁻²⁹

The results presented here are similar to previous reports using 2D PET in terms of sensitivity, specificity and accuracy, as illustrated in Figure 6. Our measured sensitivity was higher than most of the other studies.^{1-4,6} One potential reason for this may be the incremental use of TID as a marker for disease. There were two patients with stenoses greater than 50% and a normal SSS (0-3), but their scans demonstrated TID (≥ 1.20). The normal SSS may be due to the fact that both had diffuse disease, which may have decreased flow to the entire myocardium. Additionally, future study may examine the use of LVEF reserve, which is the difference between stress and rest ejection fraction, proposed as a marker of extensive disease.³⁰ Our results are also similar to those reported recently using 3D PET-CT, but using a different scanner (Siemens Biograph) and analysis software (Cedars QPET) technologies.⁶ Our results emphasize the effects that selection criteria and LLK patients have on the results for studies examining accuracy. When patients with a history of intervened MI and LVEF < 40% are included in the patient population and LLK patients are not included, specificity appears quite low, around 50% for both 50% and 70% stenosis, which then dramatically increases after including LLK patients. This is consistent with previous studies that used minimal exclusion criteria and showed dramatic increases in specificity when LLK patients were included in the calculation (Table 2). The first of these by Esteves et al,³ using a 50% stenosis cutoff, demonstrated an increase in specificity from 50% to 76% when using a normal database, while Santana et al,² using a 70% stenosis, demonstrated an increase in specificity from 54% to 69%. Similarly, the effect of exclusion criteria can be seen in a recent

paper which did not include LLK patients in specificity calculations, but had more strict exclusion criteria.⁶ This paper reported specificity of 86% and 77% for 50% and 70% stenosis, which is similar to our reported specificity of 71% for both 50% and 70% stenosis. Including LLK patients for this same study again demonstrates a dramatic improvement in specificity, increasing to 95% and 90% for 50% and 70% stenosis, respectively.

A low-dose 10 MBq/kg, 30-second constant-activity-rate infusion was used in the present study, as opposed to relatively high-dose 2,220 MBq, 50 mL/minute constant-flow-rate bolus infusions used in previous studies.¹⁻⁶ Consistent administration of rubidium activity by weight, with consistent timing and profile regardless of the generator age in the present study resulted in a very reproducible number of recorded counts (56 ± 14 million) and image quality and across all scans. Previous studies using constant-flow-rate infusions have noted some variability in recorded counts, image quality and contrast,^{8,31} that may result from longer infusion times typically required as the generator activity decreases with age. Future investigations may determine whether variable infusion times, profiles, counts and image contrast affect the results reported here.

One potential limitation of including the LLK patients is the criticism that specificity may be artificially inflated. However, because most patients with normal PET scans are not referred to coronary angiography, this referral bias is known to influence the calculation of the true negative fraction.³² The 36 LLK patients (34% of patient sample) were included in the calculation of specificity because normalcy can serve as a proxy for specificity in the presence of post-test referral bias, which likely occurred in this study population. The inclusion of LLK validation normals in the present study is consistent with previous publications evaluating PET myocardial perfusion imaging accuracy, which included 24%¹ and 37%⁴ LLK normal subjects, respectively.

CONCLUSION

This study demonstrates that a normal database containing the relative perfusion scores of patients without obstructive CAD can be used to accurately diagnose obstructive CAD using low-dose Rb-82 with 3D PET-CT imaging. This type of semiquantitative analysis using a normal database may be useful as an adjunct to the standard visual clinical interpretation of myocardial perfusion.

Acknowledgments

This study was supported by an operating grant from the Canadian Institute of Health Research (CIHR) for the

Rb-ARMI trial (Grant MIS-100935). The study was also supported in part by the Molecular Function and Imaging (MFI) Program Grant from the Heart and Stroke Foundation of Ontario (Grant #PRG6242). R.S.B. is a Career Investigator supported by the HSFO. T.K. was supported in part by the University of Ottawa Undergraduate Research Opportunities Program. The authors would like to thank May Aung and Kimberly Gardner for acquisition of the rubidium PET-CT scans; Judy Etele for patient enrolment and consent; and Ann Guo for assistance with the statistical assessments.

Disclosure

RSB and RdK are consultants with Jubilant DRAXimage and have received grant funding from a government/industry program (partners: GE Healthcare, Nordion, Lantheus Medical Imaging, DRAXimage). RdK receives revenues from rubidium generator technology licensed to Jubilant DRAXimage. RSB is a consultant for Lantheus Medical Imaging.

References

- Bateman TM, Heller GV, McGhie AI, Friedman JD, Case JA, Bryngelson JR, et al. Diagnostic accuracy of rest/stress ECG-gated Rb-82 myocardial perfusion PET: Comparison with ECG-gated Tc-99m sestamibi SPECT. *J Nucl Cardiol* 2006;13:24-33.
- Santana CA, Folks RD, Garcia EV, Verdes L, Sanyal R, Hainer J, et al. Quantitative (82)Rb PET/CT: Development and validation of myocardial perfusion database. *J Nucl Med* 2007;48:1122-8.
- Esteves FP, Nye JA, Khan A, Folks RD, Halkar RK, Garcia EV, et al. Prompt-gamma compensation in Rb-82 myocardial perfusion 3D PET/CT. *J Nucl Cardiol* 2010;17:247-53.
- Sampson UK, Dorbala S, Limaye A, Kwong R, Di Carli MF. Diagnostic accuracy of rubidium-82 myocardial perfusion imaging with hybrid positron emission tomography/computed tomography in the detection of coronary artery disease. *J Am Coll Cardiol* 2007;49:1052-8.
- Marwick TH, Shan K, Patel S, Go RT, Lauer MS. Incremental value of rubidium-82 positron emission tomography for prognostic assessment of known or suspected coronary artery disease. *Am J Cardiol* 1997;80:865-70.
- Nakazato R, Berman DS, Dey D, Le Meunier L, Hayes SW, Fermin JS, et al. Automated quantitative Rb-82 3D PET/CT myocardial perfusion imaging: Normal limits and correlation with invasive coronary angiography. *J Nucl Cardiol* 2011; doi: 10.1007/s12350-011-9496-3.
- Schepis T, Gaemperli O, Treyer V, Valenta I, Burger C, Koepfli P, et al. Absolute quantification of myocardial blood flow with ¹³N-ammonia and 3-dimensional PET. *J Nucl Med* 2007;48:1783-9.
- Knesaurek K, Machac J, Krynycky B, Almeida O. Comparison of 2-dimensional and 3-dimensional ⁸²Rb myocardial perfusion PET imaging. *J Nucl Med* 2003;44:1350-6.
- de Kemp RA, Yoshinaga K, Beanlands RS. Will 3-dimensional PET-CT enable routine quantification of myocardial blood flow? *J Nucl Cardiol* 2007;14:380-97.
- Van Train KF, Maddahi J, Berman DS, Kiat H, Areeda J, Prigent F, et al. Quantitative analysis of tomographic stress thallium-201 myocardial scintigrams: A multicenter trial. *J Nucl Med* 1990; 31:1168-79.
- Van Train KF, Areeda J, Garcia EV, Cooke DC, Maddahi J, Kiat H, et al. Quantitative same-day rest-stress technetium-99m-

- sestamibi SPECT: Definition and validation of stress normal limits and criteria for abnormality. *J Nucl Med* 1993;34:1494-502.
12. Van Train KF, Garcia EV, Maddahi J, Areeda J, Cooke C, Kiat HS, et al. Multicenter trial validation for quantitative analysis of same-day rest-stress technetium-99m-sestamibi myocardial tomograms. *J Nucl Med* 1994;35:609-18.
 13. Parkash R, de Kemp RA, Ruddy TD, Kitsikis A, Hart R, Beauchesne L, et al. Potential utility of rubidium 82 PET quantification in patients with 3-vessel coronary artery disease. *J Nucl Cardiol* 2004;11:440-9.
 14. Morise AP. Comparison of the Diamond-Forrester method and a new score to estimate the pretest probability of coronary disease before exercise testing. *Am Heart J* 1999;138:740-5.
 15. Diamond GA, Forrester JS. Analysis of probability as an aid in the clinical diagnosis of coronary artery disease. *N Engl J Med* 1979;300:1350-8.
 16. Ziadi MC, de Kemp RA, Williams KA, Guo A, Chow BJ, Renaud JM, et al. Impaired myocardial flow reserve on rubidium-82 positron emission tomography imaging predicts adverse outcomes in patients assessed for ischemia. *J Am Coll Cardiol* 2011;58:740-8.
 17. Klein R, Adler A, Beanlands RS, de Kemp RA. Precision-controlled elution of a $^{82}\text{Sr}/^{82}\text{Rb}$ generator for cardiac perfusion imaging with positron emission tomography. *Phys Med Biol* 2007;52:659-73.
 18. Klein R, Renaud JM, Ziadi MC, Thorn SL, Adler A, Beanlands RS, et al. Intra- and inter-operator repeatability of myocardial blood flow and myocardial flow reserve measurements using rubidium-82 PET and a highly automated analysis program. *J Nucl Cardiol* 2010;17:600-16.
 19. Dilsizian V, Bacharach SL, Beanlands RS, Bergmann SR, Delbeke D, Gropler RJ. ASNC imaging guidelines for nuclear cardiology procedures: PET myocardial perfusion and metabolism clinical imaging. *J Nucl Cardiol* 2009;16:651-81.
 20. Ficaro EP, Lee BC, Kritzman JN, Corbett JR. Corridor4DM: The Michigan method for quantitative nuclear cardiology. *J Nucl Cardiol* 2007;14:455-65.
 21. Mazzanti M, Germano G, Kiat H, Kavanagh PB, Alexanderson E, Friedman JD, et al. Identification of severe and extensive coronary artery disease by automatic measurement of transient ischemic dilation of the left ventricle in dual-isotope myocardial perfusion SPECT. *J Am Coll Cardiol* 1996;27:1612-20.
 22. Hachamovitch R, Kang X, Amanullah AM, et al. Prognostic implications of myocardial perfusion single photon emission computed tomography in the elderly. *Circulation* 2009;120:2163-5.
 23. Herzog BA, Husmann L, Kaufmann PA, et al. Long-term prognostic value of ^{13}N -ammonia myocardial perfusion PET: Added value of coronary flow reserve. *J Am Coll Cardiol* 2009;54:150-6.
 24. Cerquiera MD, Weissman NJ, Dilsizian V, Jacobs AK, Kaul S, Laskey WK, et al. Standardized myocardial segmentation and nomenclature for tomographic imaging of the heart: A statement for healthcare professionals from the Cardiac Imaging Committee of the Council on Clinical Cardiology of the American Heart Association. *Circulation* 2002;105:539-42.
 25. Eng J. ROC analysis: Web-based calculator for ROC curves. Baltimore: Johns Hopkins University. Updated 2006 May 17; cited 17 Jan 2012. <http://www.jrocf.it.org>.
 26. Klocke FJ, Baird MG, Lorell BH, Bateman TM, Messer JV, Berman DS, et al. ACC/AHA/ASNC Guidelines for the clinical use of cardiac radionuclide imaging—Executive summary. *J Am Coll Cardiol* 2003;42:1318-33.
 27. Yoshinaga K, Katoh C, Manabe O, Klein R, Naya M, Sakakibara M, et al. Incremental diagnostic value of regional myocardial blood flow quantification over relative perfusion imaging with generator-produced rubidium-82 PET. *Circ J* 2011;75:2628-34.
 28. Ziadi MC, deKemp RA, Williams K, Guo A, Renaud JM, Chow BJ, et al. Does quantification of myocardial flow reserve using Rubidium-82 positron emission tomography facilitate detection of multivessel coronary artery disease? *J Nucl Cardiol* 2012; doi: 10.1007/s12350-011-9506-5.
 29. Lortie M, Beanlands RS, Yoshinaga K, Klein R, DaSilva JN, de Kemp RA. Quantification of myocardial blood flow with 82Rb dynamic PET imaging. *Eur J Nucl Med Mol Imaging* 2007; 34:1765-74.
 30. Dorbala S, Vanagala D, Sampson U, Limaye A, Kwong R, Di Carli MF. Value of vasodilator left ventricular ejection fraction reserve in evaluating the magnitude of myocardium at risk and the extent of angiographic coronary artery disease: A 82Rb PET/CT study. *J Nucl Med* 2007;48:349-58.
 31. Tang J, Rahmim A, Lautamaki R, Lodge MA, Bengel FM, Tsui BMW. Optimization of Rb-82 PET acquisition and reconstruction protocols for myocardial perfusion defect detection. *Phys Med Biol* 2009;54:3161-71.
 32. Rozanski A, Diamond GA, Berman D, Forrester JS, Morris D, Swan HJ. The declining specificity of exercise radionuclide ventriculography. *N Engl J Med* 1983;309:518-22.